



**HAL**  
open science

## Using water stable isotopes in the unsaturated zone to quantify recharge in two contrasted infiltration regimes

Florent Barbecot, Sophie Guillon, Eric Pili, Marie Larocque, E. Gibert, Jean-François Hélie, Aurélie Noret, Caroline Plain, Vincent Schneider, Alexandra Mattei, et al.

### ► To cite this version:

Florent Barbecot, Sophie Guillon, Eric Pili, Marie Larocque, E. Gibert, et al.. Using water stable isotopes in the unsaturated zone to quantify recharge in two contrasted infiltration regimes. *Vadose Zone Journal*, 2018, 17 (1), pp.1-13. 10.2136/vzj2017.09.0170 . hal-01856039v1

**HAL Id: hal-01856039**

**<https://cnrs.hal.science/hal-01856039v1>**

Submitted on 28 Nov 2022 (v1), last revised 11 Oct 2018 (v2)

**HAL** is a multi-disciplinary open access archive for the deposit and dissemination of scientific research documents, whether they are published or not. The documents may come from teaching and research institutions in France or abroad, or from public or private research centers.

L'archive ouverte pluridisciplinaire **HAL**, est destinée au dépôt et à la diffusion de documents scientifiques de niveau recherche, publiés ou non, émanant des établissements d'enseignement et de recherche français ou étrangers, des laboratoires publics ou privés.



Distributed under a Creative Commons Attribution - NonCommercial - NoDerivatives 4.0 International License

# Using water stable isotopes in the unsaturated zone to quantify recharge in two contrasted infiltration regimes

Florent Barbecot<sup>1</sup>, Sophie Guillon<sup>1,2</sup>, Eric Pili<sup>3</sup>, Marie Larocque<sup>1</sup>, Elisabeth Gibert-Brunet<sup>4</sup>, Jean-François Hélie<sup>1</sup>, Aurélie Noret<sup>4</sup>, Caroline Plain<sup>5</sup>, Vincent Schneider<sup>6</sup>, Alexandra Mattei<sup>1,2</sup>, Guillaume Meyzonnat<sup>1</sup>.

<sup>1</sup>GEOTOP, Département des sciences de la Terre et de l'atmosphère - Université du Québec à Montréal, CP8888 succ. Centre-Ville, Montréal, QC, H3C 3P8, Canada

<sup>2</sup>Mines ParisTech, PSL University, Centre for geosciences and geoen지니어ing, 35 rue Saint-Honoré, 77300 Fontainebleau, France

<sup>3</sup>CEA, DAM, DIF, F-91297 Arpajon, France

<sup>4</sup>UMR8148 GEOPS CNRS/UPS, Université Paris-Sud/Paris-Saclay, Bâtiment 504, 91405 Orsay Cedex, France

<sup>5</sup>UMR EEF-UL1137, INRA/Université de Lorraine, Bld des Aiguillettes, BP 239, 54506 Vandœuvre-lès-Nancy, France

<sup>6</sup>ANDRA - Centre de stockage de l'Aube, DOI/CA/QED, 10200 Soullaines-Dhuys, BP7, France

## Core Ideas

Soil water stable isotope profiles can be used to quantify groundwater recharge

Climate conditions are recorded in water stable isotope profiles of the unsaturated zone

Soil water isotope profiles provide insight into the seasonality of recharge events

## Abstract

A reliable estimate of recharge is needed for the sustainable management of groundwater resources.

Water stable isotope ( $\delta^{18}\text{O}$  and  $\delta^2\text{H}$ ) profiles in the unsaturated zone are frequently used to quantify groundwater recharge, based on the seasonality of water isotopic compositions in precipitation. A

very simple approach consists of integrating soil water content between peak values of soil water isotopic compositions, typically corresponding to precipitation signatures from warm and cold

seasons. When precipitation isotopic compositions are available, a conceptual surface water isotopes budget and lumped parameter dispersion model can be computed. These models were

applied on two field sites with similar permeable soils with grass cover but contrasting recharge regimes and seasonality: one in the Paris Basin (France) with continuous recharge from autumn to

spring, and another in the St. Lawrence Lowlands (Quebec, Canada) with episodic recharge in fall and after snowmelt. For the two sites, the peak to peak method and isotope surface budget led to

comparable recharge intensities. At least at the Paris Basin site, evaporation is shown to slightly modify the average unsaturated zone and hence groundwater isotope composition. The proposed

parameterization of isotope fractionation due to evaporation allows qualitative estimation of the fraction of evaporation, at least during the recharge seasons. In spite of its simplifications and

limitations, the proposed parsimonious model can give estimates of recharge in a variety of sites

38 even if they are not well characterized, as it benefits from the large availability of monthly isotopic  
39 compositions in precipitation.  
40

## 41 **1. Introduction**

42 The UNESCO World Water Assessment Program identified a gap in knowledge on the impact of  
43 climate change on groundwater resources. While numerous recent studies have attempted to bridge  
44 this gap, they have also demonstrated that we currently do not have the ability to quantitatively  
45 predict the impact of climate change on groundwater resources with a satisfying degree of  
46 confidence (Crosbie et al., 2013, Kurylyk and MacQuarrie, 2013). Recharge is a key parameter in  
47 groundwater management, and thus a reliable estimate of recharge is necessary for sustainable  
48 groundwater resource development (Rivard et al., 2014). To achieve accurate water budgets,  
49 recharge quantification has been investigated at local scales using lysimeters (Pflutschinger et al.,  
50 2012, Xu and Chen, 2005), water-table fluctuations (Hagedorn et al., 2011, Healy and Cook, 2002,  
51 Liang and Zhang, 2012), and baseflow analysis (McCallum et al., 2014). Independently of the  
52 method, the impact of all possible environmental stresses, meteorological variability, and changes  
53 in climate, land use, and water extraction on the recharge regime cannot be completely taken into  
54 account (Kurylyk and MacQuarrie, 2013).

55 Variability in the stable isotope signature of soil pore water collected at depths with suction  
56 lysimeters has been used to investigate subsurface processes (Darling and Bath, 1988, Stumpp et al.,  
57 2009a, 2009b, Thomas et al., 2013). As an alternative method, water stable isotopes in the  
58 unsaturated zone offer a time-integrated fingerprint of recharge and of subsurface water pathways  
59 (Darling and Bath, 1988, Bengtsson et al., 1987, Koeniger et al., 2016). Unsaturated zone stable  
60 isotope profiles under temperate climate conditions have thus been used to study groundwater  
61 recharge mechanisms (Lee et al., 2007, Li et al., 2007, McConville et al., 2001, Mueller et al., 2014,  
62 Saxena, 1984, Song et al., 2009, Stumpp and Hendry, 2012, 2009a, 2009b). Suction lysimeters are  
63 quite time consuming to employ, with a sampling effort of at least one year, while cryogenic  
64 extraction of soil water allows the collection of comparable stable isotope data within one or a few  
65 field work days. New, faster methods, such as direct equilibration, are also becoming widely used,  
66 and raised issues regarding the possible biases between the various methods of soil water isotope  
67 analysis employed (Orlowski et al., 2016).

68 The isotopic composition of precipitation is strongly correlated with air temperature. A distinct  
69 seasonal pattern therefore occurs in precipitation under temperate climates, with summer rainfall  
70 enriched in heavy isotopes and winter rainfall depleted (Rozanski et al., 1993). In addition to  $\delta^{18}\text{O}$   
71 and  $\delta^2\text{H}$ ,  $\text{lc-excess}$  values (Landwehr and Coplen, 2004) are very sensitive to local evaporation and  
72 associated isotope fractionation occurring at the surface. These are therefore used in addition to  
73  $\delta^{18}\text{O}$  and  $\delta^2\text{H}$  to evaluate recharge processes and apparent mean residence times of soil water (Lee  
74 et al., 2007).

75 Even if transpiration predominates under temperate climates and is considered to not fractionate  
76 water stable isotopes, evaporation from plant interception or from the upper soil leads to  
77 fractionation and enrichment in heavy isotopes (Braud et al., 2005, 2009a, Sprenger et al., 2016,  
78 Sutanto et al., 2012). Water recharging during a given season can therefore be identified in deep  
79 unsaturated zone profiles, and recharge rates can be obtained from the displacement between  
80 successive seasonal inputs (Gehrels et al., 1998, Maloszewski et al., 2006, Maloszewski and Zuber,  
81 1993, McConville et al., 2001, Saxena, 1984). On the one hand, this simple peak-shift method is  
82 easily applied (Adomako et al., 2010), even if isotopic compositions of precipitation are not  
83 available (Gehrels et al., 1998). On the other hand, numerical models, such as SiSPAT-Isotopes  
84 (Braud et al 2005, 2009b), Soil-Litter-Iso (Haverd et al., 2010) or a modified version of HYDRUS-  
85 1D (Stumpp et al., 2009a, 2009b, 2012), are increasingly being used to understand the dynamics of  
86 water stable isotopic composition in the unsaturated zone (Sprenger et al., 2015). Such level of  
87 model refinement is associated with high data requirement that can only be achieved for specific  
88 study sites, but less for more numerous and less known sites at the regional scale where there is a  
89 lack on recharge rates estimation.

90 The aim of this study is to apply a simple and parsimonious method to quantify the rate and  
91 seasonal pattern of recharge, based on water stable isotope depth profiles, applicable to sites under  
92 contrasted climate conditions, and requiring limited amount of additional data. First, the two study  
93 sites are presented, in the Paris Basin (France) and in the St. Lawrence Lowlands (Quebec, Canada),  
94 including water stable isotopic compositions of both precipitation and the unsaturated zone for each.  
95 Recharge is then calculated based on a simple peak-shift approach. A model coupling a surface  
96 water and isotope budget to a lumped parameter model is proposed for a more robust quantification  
97 of recharge, but also to explain the evolution of water isotopic composition in the unsaturated zone,  
98 and particularly to discuss the influence of evaporation.

## 99 **2 Materials and methods**

### 100 **2.1 Study sites and sampling**

#### 101 **2.1.1 The Paris Basin site (PB)**

102 The Paris Basin site (PB) is located 35 km south of Paris (France), in the very fine and well-sorted  
103 sands of the Oligocene Fontainebleau aquifer. This regional unconfined aquifer has a maximum  
104 thickness of 50-70 m. The total porosity of the aquifer is 25-40%, with volumetric water content in  
105 the unsaturated zone in the range of 7-28 vol% (Schneider, 2005). The hydraulic conductivity  
106 reaches  $1 \cdot 10^{-5}$  to  $6 \cdot 10^{-5}$  m/s (Corcho Alvarado et al., 2007, Renard and Tognelli, 2016).

107 This study site is covered with grass, with a 60 cm-thick sandy soil layer overlying a clayey-sand  
108 layer from 60 to 100 cm depth, and homogeneous sands below 100 cm (Figure 1a). In May 2006, a  
109 3 m-deep trench was dug in the unsaturated zone using an excavator. Soil sampling for pore water  
110 extraction and isotopic analysis was conducted immediately after opening the trench. Soil was  
111 sampled using a spatula, with a 2.5 cm spacing from 0 to 137 cm depth, and a 10 cm spacing from  
112 140 to 280 cm depth (Figure 1a). Soil samples weighting on average 100 g were collected in  
113 polypropylene bottles, and were stored in these air-tight bottles until stable isotope analysis.  
114 Gravimetric water content was measured on the grab samples and converted into volumetric water  
115 content assuming a bulk density of  $1500 \text{ kg m}^{-3}$ .  
116 The water table below the site lies on average 6 to 8 m below the surface. Several groundwater  
117 samples were collected from nearby wells for stable isotope analysis.  
118 Meteorological data, precipitation and temperature, were obtained with a 15 day time step from the  
119 nearby Trappes station (Meteo France). The average annual precipitation is 668 mm/yr, while  
120 average monthly temperatures fluctuate between 0 and 25 °C. An average recharge rate of 100 to  
121 150 mm/yr was calculated for the previous decades based on environmental tracers and at the  
122 regional scale around the study site (Corcho Alvarado et al., 2007) (Table 1), and confirmed by  
123 hydrological modelling in the Fontainebleau Sands (Renard and Tognelli, 2016).  
124 Precipitation was collected 10 km away, at the GEOPS laboratory (Université Paris-Sud/Paris-  
125 Saclay, Orsay, France), from August 2002 to July 2012, using paraffin oil to prevent evaporation of  
126 water in the collector and isotopic fractionation. Cumulated bulk precipitation was sampled twice a  
127 month, and its isotopic composition was measured (Figures 2-4). d-excess ( $d\text{-exc} = \delta^2\text{H} - 8 \delta^{18}\text{O}$ ) in  
128 precipitation was calculated to look for variable origins of air masses. The Local Meteoric Water  
129 Line (LWML) was defined based on isotopic composition of precipitation. Its equation ( $\delta^2\text{H} = a$   
130  $\delta^{18}\text{O} + b$ ) was used to calculate lc-excess values ( $lc\text{-exc} = \delta^2\text{H} - a \delta^{18}\text{O} - b$ ) for the soil pore water  
131 profile.

132

### 133 **2.1.2 The St. Lawrence Lowlands site (SLL)**

134 The St. Lawrence Lowlands site (SLL) is located 70 km southwest of Montreal, in the Vaudreuil-  
135 Soulanges area (Quebec, Canada), and in the medium sands of the Saint-Télésphore esker. These  
136 glacio-fluvial sediments can reach up to 40 m thickness, and lie above the regional bedrock aquifer  
137 (Larocque et al., 2015). The aquifer is locally unconfined, with a total porosity of 40%, and a  
138 hydraulic conductivity on the order of  $10^{-5}$  to  $10^{-4}$  m/s. The study site is located in a flat area close  
139 to a sand quarry. The area is covered mainly by woodland, except on the site outcrops where the  
140 soil is covered with grass and where the unsaturated zone was sampled.

141 Taking advantage of an outcrop recently exposed on the border of the sandpit excavation, the entire  
142 unsaturated zone was sampled in May 2013, for the measurement of water content and pore water  
143 isotopic composition. The vertical outcrop was refreshed immediately before sampling, by  
144 removing the 5 to 10 cm of sand exposed to the atmosphere. Sand samples were taken using a  
145 spatula, with a 5 cm spacing below the soil surface down to a depth of 2.5 m, and then a 10 cm  
146 spacing down to the water table at 4.5 m depth (Figure 1b). Soil samples weighted on average 100  
147 g, and were stored in air-tight polypropylene bottles until stable isotope analysis. The sand was  
148 homogeneous over the whole depth profile. Gravimetric water content was measured on the grab  
149 samples and converted into volumetric water content assuming a bulk density of  $1500 \text{ kg m}^{-3}$ . Daily  
150 weather data (minimum and maximum temperature, and precipitation) were obtained from the  
151 Coteau du Lac station (<http://www.mddelcc.gouv.qc.ca/climat/donnees/index.asp>), 20 km from the  
152 study site. Average annual precipitation in this area for the period 1980-2010 is 960 mm/yr  
153 (Larocque et al., 2015), with average monthly temperatures ranging from -11 to 23°C. An average  
154 recharge rate of 189 mm/yr was calculated for the period 1990-2010 using a regional surface water  
155 budget (Larocque et al., 2015) (Table 1).

156 Monthly isotopic composition values and precipitation amounts were obtained from the closest  
157 station of the GNIP network ([http://www-naweb.iaea.org/naweb/ih/IHS\\_resources\\_gnip.html](http://www-naweb.iaea.org/naweb/ih/IHS_resources_gnip.html)),  
158 namely Ottawa, from January 2010 to June 2012 (Figure 4). Even though Ottawa is relatively far  
159 (130 km) from the study site, the climate is similar at Ottawa and the SLL site, with similar average  
160 temperatures and precipitations as well as altitude, and Ottawa precipitation isotope compositions  
161 can thus be used for the SLL site model. Discrete snowpack and rain samples were collected at SLL  
162 for measurement of isotope composition, in 2012 and 2013. As for PB, the LMWL was determined  
163 and used to calculate the lc-excess for the soil pore water profile.

164

## 165 **2.2 Water extraction and isotopic analysis**

166 Stable isotopic analysis of soil pore water was conducted on water extracted from the collected soil  
167 samples using cryogenic vacuum extraction. As soils sampled for this study were mainly of sand  
168 type and relatively wet, water isotope composition from cryogenic extraction can be assumed to  
169 have limited bias. A small soil sample of around 100 grams for PB (resp. 40 g for SLL) was  
170 introduced into a vacuum line. Pore water was extracted during 6h for PB (resp. 2h for SLL) and  
171 condensed in a collection tube maintained in liquid nitrogen (Araguás-Araguás et al., 1995). The  
172 soil sample was heated around 60 °C during the extraction, under a vacuum around  $10^{-3}$  mbar. After  
173 extraction, the soil sample was weighed, heated overnight at 100 °C, and then re-weighed to  
174 determine the water extraction yield, as well as the initial soil water content.

175 The isotopic signature of water condensed in the collection tube was shown to follow a Rayleigh  
 176 distillation curve (data not shown), and more than 98% of pore water must be extracted to ensure  
 177 the absence of isotopic fractionation in the pore water sample. For this study, extraction yields were  
 178 monitored to be above 98% for all samples.

179 Oxygen and hydrogen isotopic compositions of the extracted soil pore water as well as of the  
 180 groundwater and precipitations were measured with a Thermo Finnigan Delta +<sup>TM</sup> isotope ratio  
 181 mass spectrometer in dual inlet mode, coupled to an equilibration bench, at GEOPS Laboratory  
 182 (Université Paris Sud, France) for PB, and on a Micromass Isoprime<sup>TM</sup> isotope ratio mass  
 183 spectrometer in dual inlet mode, coupled to an Aquaprep<sup>TM</sup> system, at GEOTOP-UQAM (Montreal,  
 184 Canada) for SLL. Each analysis required 200 µl of water, equilibrated at 40°C for 7 hours with CO<sub>2</sub>  
 185 for δ<sup>18</sup>O, and equilibrated at 40°C for 4 hours with H<sub>2</sub> with a platinum catalyst for δ<sup>2</sup>H.

186 Raw data were corrected using three internal working water standards, expressed in δ notation and  
 187 normalized to the VSMOW-SLAP scale:

$$188 \quad \delta^{18}\text{O} = \frac{R_{\text{sample}}}{R_{\text{VSMOW}}} - 1, \text{ where } R_i = \left( \frac{[^{18}\text{O}]}{[^{16}\text{O}]} \right)_i \quad (1)$$

189 Where *i* corresponds to sample or VSMOW. Hydrogen isotopic composition is expressed similarly  
 190 to δ<sup>2</sup>H, with  $R_i = ([^2\text{H}]/[^1\text{H}])_i$ . δ<sup>18</sup>O and δ<sup>2</sup>H are reported in ‰ versus the VSMOW international  
 191 standard. The precision of liquid water analysis (1σ) was 0.05 ‰ for δ<sup>18</sup>O, and 1 ‰ for δD. To  
 192 check that the uncertainty due to cryogenic extraction was small, dried soil samples were rewetted  
 193 with standard water. The measured isotopic composition for the extracted water was equal to that of  
 194 the standard water in the range of the analytical precision of the liquid water analysis.

195

196

### 197 **2.3. Recharge estimation from water isotope profiles in the unsaturated zone**

198 The seasonal variation in isotopic composition of precipitation (Figure 2), combined with a seasonal  
 199 pattern of evapotranspiration, were both directly linked to atmospheric temperatures. This led to a  
 200 seasonal pattern of the amount and isotopic composition of infiltration and recharge. Even if the  
 201 input function (i.e., rain isotopic composition) was unknown, a simple interpretation of water stable  
 202 isotope depth profiles would allow the amount and periods of recharge to be quantified. The  
 203 successive recharge seasons (summer/autumn vs. winter/spring) were identified in water isotope  
 204 profiles in the unsaturated zone due to their contrasting water isotopic compositions (enriched  
 205 versus depleted in heavy isotopes) (Figures 2, 5 and 6). The amount of recharge *R* (in m/yr) that  
 206 occurred during a certain time period *T* (in yr) was obtained by integrating the volumetric water



207 content  $\theta_w(z)$  over the depth interval  $[Z_1, Z_2]$  (in m), corresponding to the time period  $T$  (equation  
208 after and Leibundgut et al., 2009) :

$$209 \quad R = \frac{\int_{Z_1}^{Z_2} \theta_w(z) \cdot dz}{T} \quad (2)$$

210 For this method, the time period could only be roughly estimated, typically to one hydrological  
211 season or one year, from the evolution of water isotope composition with depth.

212

213

## 214 **2.4. Lumped parameter models for water isotopic composition in the unsaturated zone**

215 In order to explain the observed evolution of water isotopic composition in the unsaturated zone, a  
216 surface water and isotopic mass balance was used, combined with a lumped parameter model for  
217 isotope transport in the unsaturated zone. The successive steps of the model, from time series of  
218 precipitation and its stable isotopic composition to the depth profile of water isotopes in the  
219 unsaturated zone, are described below.

220

### 221 **2.4.1. Water budget at the subsurface**

222 As a reference point from which to discuss the water budget at the surface, the traditional  
223 Thornthwaite method (Thornthwaite, 1948) was used to calculate the potential recharge fluxes. This  
224 conceptual box model applied to the soil layer from the surface to the root depth, according to:

$$225 \quad P(i) = ET(i) + R(i) + I(i) + (S(i) - S(i - 1)) \quad (3)$$

226 Where  $i$  is the time step,  $P$  is precipitation (rain),  $ET$  is actual evapotranspiration,  $R$  is surface and  
227 subsurface runoff,  $I$  is percolation below the root depth i.e. recharge, and  $S$  is soil storage, all  
228 expressed in mm.

229 This water budget was calculated at the smallest time step available for stable isotopes in  
230 precipitation (15 days for PB; one month for SLL). Potential evapotranspiration (PET) was  
231 calculated following Turc (1961). Even if it was shown to tend to underestimate evapotranspiration  
232 (Fisher et al., 2013), this method was originally developed for a monthly time step, close to the one  
233 used here, and could be applied solely with temperature data, hence well adapted for poorly  
234 instrumented sites. For both PB and SLL sites, surface and subsurface runoff was assumed to be  
235 negligible due to the flat topography and very permeable sandy soils. The conceptual soil storage  
236 reservoir, with a maximum capacity  $S_{max}$ , corresponded to the upper soil down to the maximum  
237 rooting depth (0.1 to 0.2 m at both sites), where evaporation and transpiration occurred, and below  
238 which there was no more water abstraction. Water “overflowing” and leaving this soil reservoir  
239 percolated vertically in the unsaturated zone and finally recharged the underlying aquifer. At each

240 time step  $i$ , precipitation  $P(i)$  and soil water  $S(i-1)$  were considered as available water for  
 241 evaporation and transpiration. Actual evapotranspiration was calculated based on the demand on  
 242 potential evapotranspiration and this amount of water available in the precipitation and soil  
 243 reservoir:  $ET(i) = \min[PET(i), S(i-1)+P(i)]$ . If some water remained available after subtraction of  
 244 the actual evapotranspiration, it was added to the soil storage. Recharge was then calculated as  
 245 overflow, water exceeding the threshold capacity  $S_{max}$  of the soil storage reservoir. This could be  
 246 summarized as  $I(i) = \max[S(i-1) + P(i) - \min[PET(i), S(i-1)+P(i)], 0]$  and  $S(i) = \max(S(i-1) + P(i)$   
 247  $- \min[PET(i), S(i-1)+P(i)], S_{max}]$ . Such simple conceptual box model was assumed valid as the  
 248 calculation time step was long, typically 15 to 30 days, and as the objective was to build a data  
 249 parsimonious model.

250 For SLL, recharge was expected to occur in autumn and with snowmelt in the spring, the soil  
 251 usually being frozen from mid-December to March. Hence, the water budget was modified, with  
 252 evapotranspiration and recharge set to zero when average monthly temperature remained below  
 253 zero. The potential excess water then accumulated in the soil reservoir until positive temperatures  
 254 occurred.

255

256

#### 257 **2.4.2. Hydro-isotopic surface budget**

258 Following the traditional surface water budget (Equation 3), a simple mass balance approach was  
 259 applied to determine the isotopic composition of percolating water. At each time step, the water  
 260 isotopic composition of the soil storage reservoir was calculated by weighting the isotopic  
 261 composition of water in the soil reservoir at the previous time step and the isotopic composition of  
 262 the precipitation at the current time step:

$$263 \quad \delta_{mix}(i) = \frac{\delta_S(i-1) \cdot S(i-1) + \delta_P(i) \cdot P(i)}{S(i-1) + P(i)} \quad (4)$$

264 where  $\delta$  is the isotopic composition of oxygen  $\delta^{18}\text{O}$  or deuterium,  $\delta^2\text{H}$ ,  $\delta_S$  and  $\delta_P$  are the isotopic  
 265 compositions of soil storage and of precipitation respectively, and  $S(i)$  and  $P(i)$  are the amounts of  
 266 water in soil storage and in precipitation respectively at time step  $i$ .

267 Partitioning between evaporation and transpiration was not included in the model, neither based on  
 268 field properties nor directly based on water stable isotopes as done by Sutanto et al. (2012).  
 269 However, for grassland under northern latitudes as for the two sites, transpiration was shown to  
 270 dominate with more than 60 to 65 % of total actual evapotranspiration (Wei et al., 2017). As will be  
 271 discussed in Section 4.4., the isotopic composition of water in the unsaturated zone was used as a  
 272 simple proxy to identify whether some evaporation occurred during the recharge period(s), without  
 273 going further into quantification. At PB, isotopic compositions clearly followed an evaporative

274 trend, with negative lc-excess (Figure 6a), while it was not the case at SLL with null or slightly  
 275 positive lc-excess (Figure 6b). In the model, isotopic fractionation was therefore assumed to occur  
 276 due to evaporation of water in the soil reservoir. Soils of the two study sites were wet (Figure 5,  
 277 water content above 10 vol%), consistent with medium intensity of evapotranspiration fluxes, and  
 278 the equations of isotopic fractionation for open water (Gonfiantini, 1986) were used, including  
 279 equilibrium fractionation as well as kinetic enrichment. At each time step, the isotopic composition  
 280 of water in soil storage was calculated by:

$$281 \quad \delta_s(i) = \left( \delta_{mix}(i) - \frac{A(T,Hr)}{B(T,Hr)} \right) \cdot f^{B(T,Hr)} + \frac{A(T,Hr)}{B(T,Hr)} \quad (5)$$

282 where  $f$  is the fraction of water remaining after evaporation, and  $A(T,Hr)$  and  $B(T,Hr)$  are  
 283 parameters defined in Gonfiantini (1986), which depend on both atmospheric temperature,  $T$ , and  
 284 atmospheric relative humidity,  $Hr$ . Following Barnes and Allison (1983), in  $A$  and  $B$  terms the  
 285 kinetic enrichment is equal to  $(1-Hr)$ , the relative difference of transport resistance in air between  
 286 isotopes being neglected.

287 The outputs of the water budget (Sect. 2.4.1., Equation (3)) were used to calculate  $\delta_{inf}(i)$ , the  
 288 isotopic composition of water percolating from soil storage into the unsaturated zone.  $\delta_{inf}(i)$  was  
 289 determined for the time steps during which recharge occurred (Figure 3), and was equal to  $\delta_s(i)$ , the  
 290 isotopic composition of water in soil storage at this same time step.

291 The model was applied to PB from January 2002 to May 2006. For SLL, the hydro-isotopic surface  
 292 budget was calculated from January 2010 to May 2013, with a monthly time step.

293

### 294 **2.4.3. Transport in the unsaturated zone: piston flow with dispersion**

295 The second step of the model was the transport of water stable isotopes through the unsaturated  
 296 zone. Considering the limited amount of data available with which to constrain the model, a  
 297 conceptual input-output lumped parameter model based on transit time distribution was chosen in  
 298 this study to identify the main processes. According to the literature (Barnes and Allison, 1988,  
 299 Lindström and Rodhe, 1992) and in agreement with the observed variability in  $\delta^{18}\text{O}$  and  $\delta^2\text{H}$  with  
 300 depth (Figure 5), transport of water stable isotopes in the unsaturated zone occurred by convection  
 301 or piston flow, as well as dispersion, leading to attenuation at depth,. The convolution integral  
 302 method of Maloszewski and Zuber (1993) was chosen to reproduce and interpret soil depth profile  
 303 data.

304 First, the amount of recharge,  $I(i)$  (Equation (3)), and the isotopic composition of the percolating  
 305 water,  $\delta_{inf}(i)$ , obtained from the water and isotope budgets as a function of time (Figure 3) were  
 306 combined and transformed into  $\delta_{inf}(q)$ , a series of isotopic compositions for each increment of  
 307 recharge water  $q$  (in mm). Water content was not constant with depth (Figure 5), but the spatial and

308 temporal variations of soil water content were not included in the model as it was intended only as a  
 309 simple model for validation of the surface budget and main recharge processes and not as an  
 310 investigation of transient processes. The assumption of homogeneous and constant water content by  
 311 volume  $\theta_w$  was done, corresponding to steady-state vertical flow of water. This assumption was  
 312 required to apply the transit time distribution model. A simple mass balance, or piston flow model,  
 313 was applied to propagate the series  $\delta_{inf}(q)$  into a series  $\delta'_{inf}(z)$  of isotopic composition as a function  
 314 of depth in the unsaturated zone. This was done using the simple conversion:

$$315 \quad z = \frac{Q_{max} - q}{\theta_w} \quad (6)$$

316 where  $z$  is the depth (in mm) reached by the parcel of water after a cumulated amount of recharge of  
 317  $q$  (in mm) and  $Q_{max}$  the cumulated recharge amount (in mm) calculated for the entire time series  
 318 (2002-2006 at PB).

319 Second, the relationship between input and output soil water isotopic compositions was based on a  
 320 transit time distribution function. The dispersion model (Maloszewski et al., 2006) was chosen as  
 321 the most appropriate for solute transport in soil columns. This dispersion model was retained also  
 322 for its parsimony, with dispersion parameter as the single parameter. However, the limitations of  
 323 this model have to be kept in mind, especially through the steady-state assumption. The model  
 324 proposed here aimed at giving a general estimate of water fluxes, not at explaining the transient  
 325 dynamics of soil water isotopes.

326 Traditionally, the dispersion model was used to determine the temporal evolution of the isotopic  
 327 composition of unsaturated zone water collected at a fixed depth with a lysimeter, based on the  
 328 temporal evolution of the isotopic composition in precipitation. For the current application, the  
 329 isotopic composition of unsaturated zone water for all depth had to be calculated at a fixed time,  
 330 namely time of sampling. The lumped parameter dispersion model was therefore modified as  
 331 follows. For each depth  $Z$ , the isotopic composition after dispersion  $\delta'_{out}(Z)$  was obtained by a  
 332 convolution between the transit time distribution function with the theoretical non attenuated depth  
 333 profile  $\delta'_{inf}(z)$  :

$$334 \quad \delta'_{out}(Z) = \int_{z=0}^{Z_{max}} \delta'_{inf}(z) \cdot g(Z, z) \cdot dz \quad (7)$$

335 where  $Z_{max} = Q_{max} / \theta_w$  (in m) is the maximum depth reached by water that recharged at the really  
 336 beginning of the time series, and  $g$  is the transit time distribution function of the dispersion model:

$$337 \quad g(z) = \frac{\sqrt{z} \cdot z^{-3/2}}{\sqrt{4\pi \cdot D}} \exp\left(-\frac{(Z-z)^2}{4D z Z}\right) \quad (8)$$

338 where  $D$  is the dispersion parameter (-), that corresponds to the inverse of the Peclet number  
 339 (Maloszewski and Zuber, 1993) and hence can theoretically be linked to dispersivity.

340 The depth profile of water content was not modeled, as it was not the main focus of the study, and  
 341 not adapted to the lumped parameter model.

342 The transport model was applied only at PB. For SLL, the surface budget was less well constrained,  
 343 due to the lack on time series on snowpack and snowmelt, and the transport segment was not  
 344 pursued.

345

#### 346 **2.4.4. Sensitivity analysis and calibration of the model parameters**

347 Four years of data were available prior to sampling at PB. The model was thus run from July 2002  
 348 to May 2006. Isotopic compositions were observed to be constant below 2 m at PB (Figure 5a).  
 349 With such dispersion the available 4-year period of data was long enough so that the first and oldest  
 350 recharged water isotopic compositions were attenuated at 2 m depth. Especially, any data older than  
 351 2002 would have been attenuated. To ensure initialization of the model but keep its simplicity, the  
 352 recharge time series,  $\delta'_{inf}(z)$ , was artificially extended into the past (corresponding to the deepest  
 353 part of the unsaturated zone) using the measured average isotopic composition of the deep  
 354 unsaturated zone. For cases where shorter time series of meteorological data were available or if  
 355 dispersion was lower, monthly average data of precipitation amounts and isotope compositions  
 356 should be used for a spin up period.

357 A simple sensitivity analysis was conducted to determine the influence of the hydro-isotopic budget  
 358 parameters on the average isotopic composition and intensity of recharge (Table 2). The value of  
 359 atmospheric relative humidity  $Hr$  did not influence much the isotopic composition of recharged  
 360 water, but controlled the slope of the unsaturated zone data points relative to the meteoric water line  
 361 in  $\delta^{18}\text{O}$ - $\delta^2\text{H}$  space. The value of  $f$  strongly influenced the isotopic composition of recharged water  
 362 (Table 2), and the value of  $S_{max}$  also influenced it, albeit to a lesser extent. The values of these three  
 363 latter parameters were determined by a simple inverse approach. The objective function  $\phi$  that was  
 364 minimized was defined as the difference between the calculated volume weighted average  $\delta^{18}\text{O}$  of  
 365 recharge water and the measured volume weighted average  $\delta^{18}\text{O}$  in the unsaturated zone:

$$366 \quad \phi = \left| \frac{\sum_i I(i) \cdot \delta_{inf}(i)}{\sum_i I(i)} - \overline{\delta^{18}\text{O}_{UZ}} \right| \quad (9)$$

367 The calibration of the two parameters of the transport model, namely the dispersion coefficient,  $D$ ,  
 368 and soil water content,  $\theta_w$ , was then performed. The transport parameter values depended on those  
 369 of the parameters obtained from the surface budget. Soil water content  $\theta_w$ , was not very sensitive  
 370 and was estimated by manual adjustment, For the dispersion coefficient, a coupled multi-parameter  
 371 calibration as in Sprenger et al. (2015) was not conducted, but rather a simple parameter adjustment  
 372 based on the minimization of the objective function  $\phi'$  defined as the sum of the differences  
 373 between the measured and calculated  $\delta^{18}\text{O}$  in the unsaturated zone at each depth where  
 374 measurement was available:

$$\varphi' = |\sum_{Z_0}^{Z_{max}} (\delta'_{out}(Z) - \delta^{18}O_{UZ}(Z))| \quad (10)$$

375  
376 The transport model applied only to water percolating below the active rooting depth. The upper 10  
377 to 20 cm of the soil, which corresponded to the conceptual soil reservoir or at least where transient  
378 surface water fluxes occurred, were thus not handled by the transport model and not considered for  
379 the fit and interpretation.

380

381

### 382 **3 Results**

#### 383 **3.1. Water budget**

384 For PB, the average annual precipitation and potential evapotranspiration were 668 mm/yr and 746  
385 mm/yr respectively. The surface water budget was calculated for a fitted  $S_{max}$  value of 52 mm,  
386 giving the best agreement for isotopic composition (see Section 3.5.). The actual evapotranspiration  
387 was 455 mm/yr, for an average recharge of 203 mm/yr (Table 1). Recharge was obtained almost  
388 continuously from September/October until April/May (Figures 2 and 3). In that case, the value of  
389  $S_{max}$  could be compared to soil moisture capacity, according to  $S_{max} = RD (\theta_{FC} - \theta_{WP})$  (Renard and  
390 Tognelli, 2016) where  $RD$  is the rooting depth (0.2 m for PB site),  $\theta_{FC}$  (resp.  $\theta_{WP}$ ) the water content  
391 of soil at field capacity (resp. at wilting point) (around 5 %, resp. 2 %). Physical soil properties gave  
392 a  $S_{max}$  value of 6 mm, which was lower but compatible with the fitted value. The obtained  
393 intensities for the various components of the water budget were in agreement with those used by  
394 Renard and Tognelli (2016) for another site nearby in the Paris Basin.

395 For SLL, the average annual precipitation (rain and snow) and potential evapotranspiration for the  
396 2010-2013 period were 922 mm/yr and 630 mm/yr respectively. The  $S_{max}$  value leading to the best  
397 agreement between modelled and measured volume weighted average isotopic composition was  
398 300 mm, a large value that could not be linked to a physical interpretation of soil moisture content.  
399 It has to be emphasized here that  $S_{max}$  was a fitting parameter of the conceptual water budget, and  
400 that the link with field observations was not straightforward, especially as  $S_{max}$  depended on the  
401 model time step. The large value of  $S_{max}$  was thus consistent with the long time step (one month) of  
402 the model at SLL. The corresponding recharge was 200 mm/yr, in the same order of magnitude as  
403 the literature value (Table 1), but occurred only for snowmelt. The actual evapotranspiration was  
404 608 mm/yr, almost equal to the potential evapotranspiration. At the regional scale, Larocque et al.  
405 (2015) obtained a lower value of 381 mm/yr, but this had to be considered carefully as they  
406 considered runoff. The water budget thus appeared to be somehow too simple to fully handle

407 processes occurring in cold climate and thus to be affected by large uncertainty. Larocque et al.  
 408 (2015) used a more complex surface water budget better adapted to cold climate and showed that  
 409 recharge occurred during two separate periods for SLL, from October to December and then from  
 410 March to May. A  $S_{max}$  value of 50 mm was also tested, similar to that for PB site. This led to an  
 411 actual evapotranspiration of 517 mm/yr and recharge of 372 mm/yr, with an acceptable fit of  
 412 isotopic composition but this time with the two expected periods of recharge.

413

414

### 415 **3.2. Stable isotopic composition of precipitation**

416 Monthly-averaged amount-weighted isotopic compositions of precipitation for the two sites are  
 417 presented in Figure 2. The entire time series of isotopic compositions and d-excess in precipitation  
 418 from 2002 to 2006 for the PB site is presented in Figure 3. A marked seasonal fluctuation existed  
 419 for both sites, due to temperature effects, with correlation coefficients ( $R^2$ ) of 0.36 and 0.60 between  
 420  $\delta^{18}\text{O}$  in precipitation and temperature for PB and SLL sites respectively. Isotopic compositions of  
 421 both oxygen and hydrogen were more depleted in heavy isotopes during winter, and more enriched  
 422 in heavy isotopes during summer. The amplitude of this seasonal fluctuation was greater for SLL  
 423 (97 ‰ for  $\delta^2\text{H}$  and 12 ‰ for  $\delta^{18}\text{O}$ ) than for PB (29 ‰ for  $\delta^2\text{H}$  and 5 ‰ for  $\delta^{18}\text{O}$ ) due to the larger  
 424 underlying temperature amplitude. For SLL, the isotopic compositions of the local rain samples  
 425 were fully consistent with the values from the GNIP station in Ottawa. The average isotopic  
 426 composition of the snow samples was  $-17.3 \pm 0.1$  ‰ for  $\delta^{18}\text{O}$  and  $-126.1 \pm 1.0$  ‰ for  $\delta^2\text{H}$ , also in  
 427 the range of the GNIP station data.

428 For both sites, the local meteoric water lines (LMWL) were close to the global meteoric water line  
 429 (Figure 4a,  $\delta^2\text{H} = 7.12 \cdot \delta^{18}\text{O} + 2.19$  for PB, Figure 4b  $\delta^2\text{H} = 7.93 \cdot \delta^{18}\text{O} + 10.1$  for SLL). They  
 430 compared well with LWML equations in the same regions (see for example Millot et al., 2010 for  
 431 PB and Arnoux et al. 2017 for SLL). For PB, the d-excess varied throughout the year according to  
 432 the variable sources of vapour masses and the continental recycling of water vapour. The lc-excess  
 433 was therefore used to overcome this variability and to investigate local evaporation effects.

434

435

### 436 **3.3. Stable isotopic composition of pore water in the unsaturated zone and of groundwater**

437 Depth profiles of the water isotopic composition in the unsaturated zone are presented in Figures 5a  
 438 and 6a for PB, and Figures 5b and 6b for SLL. Only  $\delta^{18}\text{O}$  profiles are reported, as  $\delta^2\text{H}$  profiles show  
 439 similar patterns of variability. At both sites, at least one cycle of pore water isotopic composition

440 variation was observed: higher isotopic compositions corresponding to recharge at the end of  
441 summer and during autumn, and lower values corresponding to recharge during winter. The  
442 amplitude of soil water isotopic composition variability was dampened compared to that of  
443 precipitation, with 12 ‰ for  $\delta^2\text{H}$  and 2 ‰ for  $\delta^{18}\text{O}$  for PB, and with 51 ‰ for  $\delta^2\text{H}$  and 7 ‰ for  $\delta^{18}\text{O}$   
444 for SLL. At PB, the 4.5 ‰  $\delta^{18}\text{O}$  amplitude in precipitation was attenuated to 1 ‰ at 1 m depth and  
445 to less than 0.1 ‰, in the range of noise, at 2 m depth. Depth profiles of soil water content also  
446 showed some variability (Figure 5), with higher water content in the finer layer at PB and at the  
447 surface at both sites, as sampling was conducted in May following winter infiltration.

448 The average isotopic composition of water in the unsaturated zone, weighted by the water content at  
449 each depth, was equal to  $\delta^{18}\text{O}_{\text{uz}} = -6.9$  ‰ and lc-excess = -3.7 ‰ for PB, and  $\delta^{18}\text{O}_{\text{uz}} = -11.3$  ‰ and  
450 lc-excess = 2.3 ‰ for SLL (Figures 5 and 6).

451 At PB, the average isotopic composition of groundwater was  $\delta^{18}\text{O} = -6.3$  ‰ and  $\delta^2\text{H} = -48.3$  ‰  
452 (Figure 4a), while the measured isotopic composition of groundwater in the regional surface aquifer  
453 of SLL was  $\delta^{18}\text{O} = -11.1$  ‰ and  $\delta^2\text{H} = -78.5$  ‰ (Larocque et al., 2015) (Figure 4b).

454 Even if the two sites had contrasted recharge seasonality and mechanisms, the average isotopic  
455 composition of the unsaturated zone was close to that of local groundwater (Figure 4). For SB, it  
456 was quite close to the weighted average isotopic composition of local precipitation, reflecting the  
457 continuous infiltration and recharge of precipitation from fall to spring. On the contrary, for SLL  
458 the average isotopic composition in the unsaturated zone was more depleted in heavy isotopes  
459 compared to the weighted average isotopic composition of local precipitation, corresponding to the  
460 large amount of heavy isotope-depleted snowmelt water infiltration as freshet. Comparison between  
461  $\delta^{18}\text{O}$  values in precipitation and in the unsaturated zone indicated that recharge occurred  
462 predominantly during late fall ( $\delta^{18}\text{O}$  around -10 ‰) and spring ( $\delta^{18}\text{O}$  of snow around -15 ‰) at SLL  
463 (Figures 2 and 5b) and more continuously during fall, winter and spring at PB (Figures 2, 3 and 5a).  
464 At PB, lc-excess values in the unsaturated zone ranged between 0 and -5 ‰ (Figure 6a), indicating  
465 that at least some evaporation occurs before or during infiltration, leading to a slight enrichment of  
466 the isotopic composition in recharge in the unsaturated zone. At SLL, average lc-excess values in  
467 the unsaturated zone were positive (Figure 6b), showing no evidence of evaporation, and suggesting  
468 existence of heterogeneity in precipitation sources between recharge and non recharge periods.

469

#### 470 **3.4. Quantification of recharge for the two contrasted sites from unsaturated zone profiles**

471 Annual amounts of recharge were calculated following Equation (2) for both the PB and SLL  
472 profiles, and are reported in Table 1. The depths between which soil water content was integrated  
473 were chosen based on the visual observations of maximum / minimum as well as smooth or more



474 abrupt changes in the isotopic composition vs. depth (Figure 5), and on the expected seasonality of  
 475 isotopic composition in recharge, from higher values in autumn to more negative values in spring.  
 476 At PB, one cycle between two minima of  $\delta^{18}\text{O}$  was identified between 22 and 160 cm depth (Figure  
 477 5a), corresponding to an annual recharge of 304 mm/yr (Table 1). More specifically, infiltration  
 478 during autumn –winter 2005 could be identified by relatively higher isotope composition between  
 479 50 and 125 cm depth, while recent infiltration in spring 2006 would lie on top of the profile, down  
 480 to 50 cm depth (Figure 5a). At SLL, relatively abrupt changes of  $\delta^{18}\text{O}$  vs. depth allowed  
 481 identification of spring snowmelt and autumn recharge for the two hydrological years preceding  
 482 sampling (Figure 5b). In the upper part of the profile, snowmelt recharge in 2013 was identified  
 483 with low  $\delta^{18}\text{O}$  values between 22 and 72 cm and amounted to 48 mm, and a recharge in autumn  
 484 2012 of 66 mm was identified with high  $\delta^{18}\text{O}$  values between 77 and 142 cm. This led to an annual  
 485 recharge of 114 mm/yr (Table 1). Below that, low  $\delta^{18}\text{O}$  are again observed from 147 to 212 cm,  
 486 corresponding to spring snowmelt in 2012, with a calculated recharge of 68 mm. Below 217 cm,  
 487  $\delta^{18}\text{O}$  values increased slightly and probably corresponded to recharge from autumn 2011, but the  
 488 amplitude of variations were too dampened to allow quantification. Quantification of recharge  
 489 based on integration of water content versus depth was based on a subjective identification of the  
 490 depth range corresponding to a given period of recharge, and thus subjected to a large uncertainty.  
 491 But the results obtained here provided a straightforward first order estimate of the amount of  
 492 recharge and also a confirmation of the expected seasonality of recharge.

493

### 494 **3.5. Modeling the isotopic composition evolution from precipitation to infiltration and** 495 **recharge**

496 For PB site, Equation (5) and isotope fractionation were at first not included in the model, but the  
 497 minimization of the objective function  $\phi$  never led to a good fit of the data (data not shown). As  
 498 already identified with the negative lc-excess value in the unsaturated zone, this confirmed that  
 499 some evaporation occurred at PB. Isotope fractionation was therefore included in the model.  
 500 Minimization of the objective function  $\phi$  then led to the determination of the surface water budget  
 501 parameters ( $S_{max}$  and evaporation parameters,  $f$  and  $Hr$ ). The best fit (Figures 5a and 6a) was  
 502 obtained for  $S_{max}=52$  mm,  $Hr=0.3$  and  $f=0.97$ . The obtained average annual recharge was then 203  
 503 mm/yr (Table 1), not fully similar to the values obtained from the depth integration method (Section  
 504 3.4) and the literature, but of the same order of magnitude and acceptable regarding the  
 505 simplifications of the model and associated uncertainties. It has to be noted that the surface hydro-  
 506 isotopic budget was self-sufficient to quantify amount and seasonality of recharge. The transport  
 507 model served as validation and confirmation of major recharge processes.

508 Regarding the lumped parameter transport model for PB, the distance between the two  $\delta^{18}\text{O}$  minima  
509 in the soil profile (Figure 5a) was compared to the amount of recharge between the two  $\delta_{inf}(r)$  series  
510 minima, and Equation (6) was used to deduce an average water content of  $\theta_w = 0.42$ . This value was  
511 higher than the field value of 0.15 to 0.25 (Figure 5a), but this parameter was not optimized  
512 automatically, was not very sensitive and thus affected by a large uncertainty. A dispersion  
513 parameter  $D$  of 0.06 gave the best fit between observed and calculated profiles (Figures 5a and 6a).  
514 This dispersion parameter was an effective bulk parameter for the whole profile, disregarding the  
515 spatial variations of dispersivity with depth, and was not interpreted in terms of dispersivity.  
516 For SLL, as already guessed by the positive lc-excess values in the unsaturated zone, a model  
517 without evaporation and without isotope fractionation allowed to minimize the objective function  
518 and was thus retained. There was thus only one parameter,  $S_{max}$ , to calibrate. The best agreement  
519 between average  $\delta^{18}\text{O}$  and  $\delta^2\text{H}$  calculated for recharge versus measured values in the unsaturated  
520 zone profile was obtained for a  $S_{max}$  of 300 mm, leading to an annual recharge of 200 mm/yr (Table  
521 1), again different from but of the order of magnitude of values obtained from the simple depth  
522 integration method (Section 3.4) and from the literature. However, as already discussed above  
523 (Section 3.1), a  $S_{max}$  value of 50 mm, similar to that for PB site and more physical, led to a higher  
524 recharge of 372 mm/yr, and emphasized the current limitations of the model for cold climate.

525

526

## 527 **4 Discussion**

### 528 **4.1. Processes to include in models of soil water isotope profiles**

529 In this study, a conceptual water isotope budget was used at the surface, based on the traditional  
530 water budget, but also taking physical processes that alter soil water isotopic composition into  
531 account, namely mixing and isotopic fractionation associated with evaporation. Regarding transport  
532 in the unsaturated zone, the choice of a lumped dispersion model to reproduce the measured  $\delta^{18}\text{O}$  in  
533 the unsaturated zone was based on the limited availability of data with which to constrain the  
534 model. The simplified surface budget was consistent with a simplified transport model that did not  
535 incorporate the variations of water content with depth and with time. The influence of soil  
536 heterogeneity as well as of immobile water on the average isotopic composition of recharge water,  
537 were considered to be negligible by several authors (Barnes and Allison, 1988, Lindström and  
538 Rodhe, 1992), but shown to occur by others (Gazis and Feng, 2004, Schoen et al., 1999). The use of  
539 a lumped parameter model allowed these processes to be taken somehow into account through the  
540 effective dispersion parameter.

541 Other modeling approaches with more physically based numerical models of surface water,  
542 isotopes, and heat budgets have been proposed, coupled with water and isotope transport in the  
543 unsaturated zone based on Richard's equation (Braud et al., 2005, Gehrels et al., 1998, Haverd and  
544 Cuntz, 2010, Melayah et al., 1996, Rothfuss et al., 2012, Sprenger et al., 2015, Stumpp et al., 2012).  
545 Such physically based models handle transient dynamics of flow and transport in the unsaturated  
546 zone as well as soil heterogeneity, and help improve the calibration of soil transport parameters and  
547 the understanding of water residence time. However, they often lack detailed presentation of surface  
548 isotope water budget. Non-fractionating transpiration is usually included in the models for sites in  
549 temperate areas (e.g. HYDRUS-1D, Stumpp et al., 2012), but isotope fractionating evaporation is  
550 less often taken into account (Haverd and Cuntz, 2010, Rothfuss et al., 2012, Sprenger et al., 2017).  
551 These modeling approaches can be more or less complex but always require many data and  
552 parameters. On the opposite, the model proposed here is much more conceptual and simplified, but  
553 includes this isotope fractionation in a simple way while requiring few data and parameters.

554

#### 555 **4.2. Parsimonious models for recharge quantification and uncertainties**

556 The two sites considered in this study have contrasted recharge mechanisms and seasonality, with  
557 episodic recharge in autumn and from snow melt at SLL, and more continuous recharge from  
558 autumn to spring at PB. The two models proposed here prove to allow quantification of recharge  
559 amount and possibly seasonality, for sites that are not so well characterized and where only limited  
560 data are available to interpret the isotope composition of pore water in the unsaturated zone.

561 The two methods give estimates of recharge intensity that are of the same order of magnitude as  
562 values given in the literature and obtained with hydrogeological modeling (Table 1). However, even  
563 if a precise quantification was not the scope of the study and uncertainties on annual recharge  
564 estimated from depth integration of water content as well as from our simple model are large,  
565 noticeable differences remain with literature values. Such uncertainties could not easily be handled  
566 by water managers, and the proposed models are not intended for their use. More generally,  
567 uncertainties on recharge estimations remain significant, especially when comparing methods and  
568 even with complex models, which emphasizes the need to further improve recharge quantification  
569 methods.

570

#### 571 **4.3. Limitations of the proposed water isotope budget and transport model for recharge** 572 **quantification**

573 The main limitation of the use of unsaturated zone water isotope profiles is the attenuation of the  
574 precipitation isotope signal at depth (Cook et al., 1992). As opposed to arid or semi arid regions

575 with deep unsaturated zone where several years of recharge intensity are stored, temperate areas  
576 generally have shallower unsaturated zone and higher recharge intensity that limits the preservation  
577 of the signals. The seasonal variability can clearly be observed at SLL, but is smaller for PB (Figure  
578 5). The model shown here is intended to be theoretically applicable to any site under a temperate  
579 climate, even if sites characterized by strong seasonality, and especially by snow cover, are better  
580 suited to the quantification of recharge from soil water isotopes profiles.

581 Another limitation of the interpretation of soil water isotope profiles is that a long-term time series  
582 of precipitation isotopic composition is required. Monthly time step time series have been used as  
583 they are more easily acquired or available from GNIP stations almost all over the world. A monthly  
584 time step is shown here to enable the application of a hydro-isotopic surface budget and the  
585 identification of seasonal variations in recharge. If associated with a soil sampling at fine spatial  
586 resolution, typically every 5 cm or so, high resolution precipitation data could allow using a two  
587 components lumped parameter model, with both piston flow and dispersion models, to investigate  
588 the existence of preferential infiltration events, as proposed by Stumpp and Maloszewski (2010).

589 Uncertainties in the surface water budget propagate also into the transport model. The major  
590 limitation of the transport model is the assumption of steady-state flow (homogeneous and constant  
591 soil water content), that is required to apply the lumped parameter dispersion model, but that  
592 prevents any investigation of transient processes.

593 Finally, the surface water budget and transport models are calibrated here on one single profile  
594 taken at one time, which is one of its strength but also a limitation as it increases the uncertainties,  
595 from sampling and cryogenic extraction to model calibration.

596 Despite these limitations, the simple surface and transport models are complementary to the peak to  
597 peak method and are applicable to sites where little information is available.

598

#### 599 **4.4. Impact of evaporation on water isotopic composition in the unsaturated zone**

600 Isotopic fractionation is associated with evaporation at the soil surface, and is known to be an  
601 important control of the isotopic composition of water in soils (Barnes and Allison, 1983, 1988,  
602 Sutanto et al., 2012). The average negative  $\delta^{18}O$ -excess value in the unsaturated zone for PB indicates  
603 the role of local evaporation, and this is confirmed by the hydro-isotopic surface budget, where  
604 isotope fractionation has to be included in order to fit the data. For SLL, this is not the case, average  
605  $\delta^{18}O$ -excess is positive and a good fit of the data is obtained without fractionation. The fitted  $f$   
606 coefficient of 0.97 for evaporation at PB might not be directly transposed into evaporation  
607 partitioning but confirms that transpiration largely dominates water uptake for soil under a  
608 temperate climate and covered with grass. Evaporation occurring during the hot summers clearly

609 leads to isotope fractionation, but as there is no recharge during summer, this fractionated signal is  
610 barely preserved in a small amount of soil moisture. When autumn rain is mixed with this small  
611 amount of fractionated water remaining in the soil reservoir, the evaporated signal is largely  
612 dampened. These values of  $f$  and evaporation therefore correspond to the recharge periods, namely  
613 autumn and spring. At SLL, where average temperatures are lower, evaporation from the  
614 unsaturated zone is negligible during the recharge seasons, spring and autumn, and hence does not  
615 impact the isotopic composition of recharge.

616 For both sites,  $l_c$ -excess appears to be a robust indicator of local evaporation intensity. Water stable  
617 isotopes in the unsaturated zone have thus already been used to partition evaporation and  
618 transpiration fluxes (Sutanto et al., 2012). Surface budgets for water stable isotopes, including  
619 fractionation associated with evaporation, as proposed in this study, should be further developed  
620 and tested under temperate climates.

621 Equation (5) is proposed as a simple parameterization of the isotope fractionation associated to  
622 evaporation in soils, but it would require improvement and validation by future experimental and  
623 numerical studies. Equation (5) is originally established for open water, and is adapted to sites such  
624 as PB where evaporation fluxes are small and kinetic fractionation is limited. Future work should  
625 focus more specifically on the validation of such isotope fractionation equation. One major issue  
626 would be to include a parameterization or a fit of a temporal evolution of the  $f$  parameter, which  
627 would require to include partitioning of evapotranspiration.

628

## 629 **5. Conclusion**

630 Based on the results from two field sites with contrasting hydrologic and climate conditions, water  
631 stable isotope ( $\delta^{18}\text{O}$  and  $\delta^2\text{H}$ ) profiles in the unsaturated zone are shown to permit the quantification  
632 and identification of seasonality in recharge, based on the seasonality of the water isotopic  
633 composition of precipitation. A very simple approach consists of integrating soil water content  
634 between extreme values of soil water isotopic composition, typically corresponding to precipitation  
635 signatures during warm and cold seasons. When a time series of precipitation isotopic composition  
636 is available, even only at a monthly time scale, a water isotope budget can be calculated at the  
637 surface using a conceptual overflowing soil reservoir model including mixing of successive  
638 precipitation but also isotope fractionation due to evaporation. The intensity of evaporation,  
639 associated with enrichment in heavy isotopes, can be constrained by the  $l_c$ -excess measured in the  
640 unsaturated zone. A first and simple parameterization is proposed to take this fractionation into  
641 account in the surface water budget. This water budget can be constrained with the volume

642 weighted average isotopic composition of pore water in the unsaturated zone, and thus allows  
643 determination of the intensity and seasonality of recharge. This model and the peak to peak  
644 integration lead to similar values, consistent at first order with more complex methods, but  
645 emphasizing the uncertainties remaining on recharge quantification. A lumped parameter dispersion  
646 model is then used to represent percolation of water and attenuation of water isotope signal at depth.  
647 It allows the main variations of water isotope composition with depth to be reproduced and soil  
648 parameters and transport processes to be discussed.

649 Even if the attenuation of the precipitation isotopic signal during recharge limits the investigation to  
650 the two first meters of the unsaturated zone and to sites with contrasted recharge periods, the  
651 approaches proposed in this study could be applied to a large number of sites, and are very  
652 promising for the investigation of spatial and temporal variability of recharge as well as for drawing  
653 recharge maps at the local to regional spatial scales.

654

#### 655 **Data availability**

656 All data are available upon request to the corresponding author.

#### 657 **Acknowledgments**

658 We thank the *Fonds de recherche du Québec – Nature et technologies* (FRQNT) and the  
659 *Programme d'acquisition de connaissances sur les eaux souterraines du Québec (PACES)* program  
660 for funding the Quebec portion of this research, as well as the *Institut de Radioprotection et Sureté*  
661 *Nucléaire* (IRSN) for assistance in collecting monthly rainfall samples. Camille Peretti and Karine  
662 Lefebvre are thanked for their help in the field and in the laboratory. We thank the Associate Editor  
663 Christine Stumpp, as well as Matthias Sprenger and an anonymous reviewer for their comments that  
664 greatly helped improving the manuscript.

665

666

#### 667 **References**

668

- 669 Adomako, D., P. Maloszewski, C. Stumpp, S. Osaé and T.T. Akiti. 2010. Estimating groundwater  
670 recharge from water isotope ( $\delta$  H-2,  $\delta$  O-18) depth profiles in the Densu River basin,  
671 Ghana. *Hydrological Sciences Journal-Journal Des Sciences Hydrologiques* 55: 1405-1416.  
672 doi:10.1080/02626667.2010.527847.
- 673 Araguás-Araguás, L., K. Rozanski, R. Gonfiantini and D. Louvat. 1995. Isotope effects  
674 accompanying vacuum extraction of soil water for stable isotope analyses. *Journal of*  
675 *Hydrology* 168: 159-171. doi:http://dx.doi.org/10.1016/0022-1694(94)02636-P.

- 676 Arnoux, M., F. Barbecot, E. Gibert-Brunet, J. Gibson, E. Rosa, A. Noret, et al. 2017. Geochemical  
677 and isotopic mass balances of kettle lakes in southern Quebec (Canada) as tools to document  
678 variations in groundwater quantity and quality. *Environmental Earth Sciences* 76.  
679 doi:10.1007/s12665-017-6410-6.
- 680 Barnes, C.J. and G.B. Allison. 1983. The distribution of deuterium and  $^{18}\text{O}$  in dry soils: 1. Theory.  
681 *Journal of Hydrology* 60: 141-156. doi:https://doi.org/10.1016/0022-1694(83)90018-5.
- 682 Barnes, C.J. and G.B. Allison. 1988. Tracing of water-movement in the unsaturated zone using  
683 stable isotopes of hydrogen and oxygen. *Journal of Hydrology* 100: 143-176.  
684 doi:10.1016/0022-1694(88)90184-9.
- 685 Bengtsson, L., R.K. Saxena and Z. Dressie. 1987. Soil water movement estimated from isotope  
686 tracers. *Hydrological Sciences Journal* 32: 497-520. doi:10.1080/02626668709491208.
- 687 Braud, I., T. Bariac, J.P. Gaudet and M. Vauclin. 2005. SiSPAT-Isotope, a coupled heat, water and  
688 stable isotope ( $\text{HDO}$  and  $\text{H}_2^{18}\text{O}$ ) transport model for bare soil. Part I. Model description  
689 and first verifications. *Journal of Hydrology* 309: 277-300.  
690 doi:https://doi.org/10.1016/j.jhydrol.2004.12.013.
- 691 Braud, I., P. Biron, T. Bariac, P. Richard, L. Canale, J.P. Gaudet, et al. 2009a. Isotopic composition  
692 of bare soil evaporated water vapor. Part I: RUBIC IV experimental set up and results.  
693 *Journal of Hydrology* 369: p. 1 - p. 16. doi:10.1016/j.jhydrol.2009.01.034.
- 694 Braud, I., T. Bariac, P. Biron and M. Vauclin. 2009b. Isotopic composition of bare soil evaporated  
695 water vapor. Part II: Modeling of RUBIC IV experimental results. *Journal of Hydrology*  
696 369: 17-29. doi:10.1016/j.jhydrol.2009.01.038.
- 697 Cook, P.G., W.M. Edmunds and C.B. Gaye. 1992. Estimating paleorecharge and paleoclimate from  
698 unsaturated zone profiles. *Water Resources Research* 28: 2721-2731.  
699 doi:10.1029/92WR01298.
- 700 Corcho Alvarado, J.A., R. Purtschert, F. Barbecot, C. Chabault, J. Rueedi, V. Schneider, et al. 2007.  
701 Constraining the age distribution of highly mixed groundwater using  $^{39}\text{Ar}$ : A multiple  
702 environmental tracer ( $^3\text{H}/^3\text{He}$ ,  $^{85}\text{Kr}$ ,  $^{39}\text{Ar}$ , and  $^{14}\text{C}$ ) study in the semiconfined  
703 Fontainebleau Sands Aquifer (France). *Water Resources Research* 43.  
704 doi:10.1029/2006WR005096.
- 705 Crosbie, R.S., B.R. Scanlon, F.S. Mpelasoka, R.C. Reedy, J.B. Gates and L. Zhang. 2013. Potential  
706 climate change effects on groundwater recharge in the High Plains Aquifer, USA. *Water*  
707 *Resources Research* 49: 3936-3951. doi:10.1002/wrcr.20292.
- 708 Darling, W.G. and A.H. Bath. 1988. A stable isotope study of recharge processes in the English  
709 Chalk. *Journal of Hydrology* 101: 31-46. doi:https://doi.org/10.1016/0022-1694(88)90026-1.
- 710 Fisher, D.K. and H.C. Pringle. 2013. Evaluation of alternative methods for estimating reference  
711 evapotranspiration. *Agricultural Sciences* 4: 51-60. doi:10.4236/as.2013.48A008.
- 712 Gazis, C. and X. Feng. 2004. A stable isotope study of soil water: evidence for mixing and preferential  
713 flow paths. *Geoderma* 119: 97-111. doi:http://dx.doi.org/10.1016/S0016-7061(03)00243-X.
- 714 Gehrels, J.C., J.E.M. Peeters, J.J. De Vries and M. Dekkers. 1998. The mechanism of soil water  
715 movement as inferred from  $\text{O}-18$  stable isotope studies. *Hydrological Sciences Journal-*  
716 *Journal Des Sciences Hydrologiques* 43: 579-594. doi:10.1080/02626669809492154.
- 717 Gonfiantini, R. 1986. Environmental isotopes in lake studies. In: P. Fritz and J. C. Fontes, editors,  
718 *Handbook of Environmental Isotope Geochemistry*. Elsevier, Amsterdam. p. 113-168.
- 719 Hagedorn, B., A.I. El-Kadi, A. Mair, R.B. Whittier and K. Ha. 2011. Estimating recharge in  
720 fractured aquifers of a temperate humid to semiarid volcanic island (Jeju, Korea) from water  
721 table fluctuations, and  $\text{Cl}$ ,  $\text{CFC-12}$  and  $^3\text{H}$  chemistry. *Journal of Hydrology* 409: 650-662.  
722 doi:http://dx.doi.org/10.1016/j.jhydrol.2011.08.060.
- 723 Haverd, V. and M. Cuntz. 2010. Soil-Litter-Iso: A one-dimensional model for coupled transport of  
724 heat, water and stable isotopes in soil with a litter layer and root extraction. *Journal of*  
725 *Hydrology* 388: 438-453. doi:doi:10.1016/j.jhydrol.2010.05.029.
- 726 Healy, R.W. and P.G. Cook. 2002. Using groundwater levels to estimate recharge. *Hydrogeology*  
727 *Journal* 10: 91-109. doi:10.1007/s10040-001-0178-0.

- 728 Koeniger, P., M. Gaj, M. Beyer and T. Himmelsbach. 2016. Review on soil water isotope-based  
729 groundwater recharge estimations. *Hydrological Processes* 30: 2817-2834.  
730 doi:10.1002/hyp.10775.
- 731 Kurylyk, B.L. and K.T.B. MacQuarrie. 2013. The uncertainty associated with estimating future  
732 groundwater recharge: A summary of recent research and an example from a small  
733 unconfined aquifer in a northern humid-continental climate. *Journal of Hydrology* 492: 244-  
734 253. doi:10.1016/j.jhydrol.2013.03.043.
- 735 Landwehr, J.M. and T.B. Coplen. 2004. Line-conditioned excess: A new method for characterizing  
736 stable hydrogen and oxygen isotope ratios in hydrologic systems. International Atomic  
737 Energy Agency (IAEA). p. 98-99.
- 738 Larocque, M., G. Meyzonnat, M.A. Ouellet, M.H. Graveline, S. Gagné, D. Barnette, et al. 2015.  
739 *Projet de connaissance des eaux souterraines de la zone de Vaudreuil-Soulanges - Rapport*  
740 *scientifique*. Ministère du Développement durable, de l'Environnement et de la Lutte contre  
741 les changements climatiques, Quebec. p. 202.
- 742 Lee, K.-S., J.-M. Kim, D.-R. Lee, Y. Kim and D. Lee. 2007. Analysis of water movement through  
743 an unsaturated soil zone in Jeju Island, Korea using stable oxygen and hydrogen isotopes.  
744 *Journal of Hydrology* 345: 199-211. doi:http://dx.doi.org/10.1016/j.jhydrol.2007.08.006.
- 745 Leibundgut, C., P. Maloszewski and C. Külls. 2009. *Tracers in Hydrology* John Wiley & Sons, Ltd,  
746 Chichester, UK.
- 747 Li, F., X. Song, C. Tang, C. Liu, J. Yu and W. Zhang. 2007. Tracing infiltration and recharge using  
748 stable isotope in taihang Mt., north China. *Environmental Geology* 53: 687-696.  
749 doi:10.1007/s00254-007-0683-0.
- 750 Liang, X. and Y.K. Zhang. 2012. A new analytical method for groundwater recharge and discharge  
751 estimation. *Journal of Hydrology* 450-451: 17-24. doi:10.1016/j.jhydrol.2012.05.036.
- 752 Lindström, G. and A. Rodhe. 1992. Transit times of water in soil lysimeters from modeling of  
753 oxygen-18. *Water, Air, and Soil Pollution* 65: 83-100. doi:10.1007/bf00482751.
- 754 Maloszewski, P., S. Maciejewski, C. Stumpp, W. Stichler, P. Trimborn and D. Klotz. 2006.  
755 Modelling of water flow through typical Bavarian soils: 2. Environmental deuterium  
756 transport. *Hydrological Sciences Journal-Journal Des Sciences Hydrologiques* 51: 298-313.  
757 doi:10.1623/hysj.51.2.298.
- 758 Maloszewski, P. and A. Zuber. 1993. Principles and practice of calibration and validation of  
759 mathematical models for the interpretation of environmental tracer data in aquifers.  
760 *Advances in Water Resources* 16: 173-190. doi:10.1016/0309-1708(93)90036-f.
- 761 McCallum, J.L., P.G. Cook, C.T. Simmons and A.D. Werner. 2014. Bias of Apparent Tracer Ages  
762 in Heterogeneous Environments. *Groundwater* 52: 239-250. doi:10.1111/gwat.12052.
- 763 McConville, C., R.M. Kalin, H. Johnston and G.W. McNeill. 2001. Evaluation of recharge in a  
764 small temperate catchment using natural and applied delta O-18 profiles in the unsaturated  
765 zone. *Ground Water* 39: 616-623. doi:10.1111/j.1745-6584.2001.tb02349.x.
- 766 Melayah, A., L. Bruckler and T. Bariac. 1996. Modeling the transport of water stable isotopes in  
767 unsaturated soils under natural conditions .1. Theory. *Water Resources Research* 32: 2047-  
768 2054. doi:10.1029/96wr00674.
- 769 Millot, R., E. Petelet-Giraud, C. Guerrot and P. Négrel. 2010. Multi-isotopic composition ( $\delta^{7}\text{Li}$ -  
770  $\delta^{11}\text{B}$ - $\delta^{\text{D}}$ - $\delta^{18}\text{O}$ ) of rainwaters in France: Origin and spatio-temporal characterization.  
771 *Applied Geochemistry* 25: 1510-1524. doi: https://doi.org/10.1016/j.apgeochem.  
772 2010.08.002.
- 773 Mueller, M.H., A. Alaoui, C. Kuells, H. Leistert, K. Meusburger, C. Stumpp, et al. 2014. Tracking  
774 water pathways in steep hillslopes by  $\delta^{18}\text{O}$  depth profiles of soil water. *Journal of*  
775 *Hydrology* 519, Part A: 340-352. doi:http://dx.doi.org/10.1016/j.jhydrol.2014.07.031.
- 776 Orłowski, N., D.L. Pratt and J.J. McDonnell. 2016. Intercomparison of soil pore water extraction  
777 methods for stable isotope analysis. *Hydrological Processes* 30: 3434-3449.  
778 doi:10.1002/hyp.10870.



- 779 Pflatschinger, H., I. Engelhardt, M. Piepenbrink, F. Königer, R. Schuhmann, A. Kallioras, et al.  
780 2012. Soil column experiments to quantify vadose zone water fluxes in arid settings.  
781 *Environmental Earth Sciences* 65: 1523-1533. doi:10.1007/s12665-011-1257-8.
- 782 Renard, F. and A. Tognelli. 2016. A new quasi-3D unsaturated-saturated hydrogeologic model of  
783 the Plateau de Saclay (France). *Journal of Hydrology* 535: 495-508.  
784 doi:http://dx.doi.org/10.1016/j.jhydrol.2016.02.014.
- 785 Rivard, C., R. Lefebvre and D. Paradis. 2014. Regional recharge estimation using multiple methods:  
786 an application in the Annapolis Valley, Nova Scotia (Canada). *Environmental Earth*  
787 *Sciences* 71: 1389-1408. doi:10.1007/s12665-013-2545-2.
- 788 Rothfuss, Y., I. Braud, N. Le Moine, P. Biron, J.-L. Durand, M. Vauclin, et al. 2012. Factors  
789 controlling the isotopic partitioning between soil evaporation and plant transpiration:  
790 Assessment using a multi-objective calibration of SiSPAT-Isotope under controlled  
791 conditions. *Journal of Hydrology* 442: 75-88.  
792 doi:https://doi.org/10.1016/j.jhydrol.2012.03.041.
- 793 Rozanski, K., L. Araguás-Araguás and R. Gonfiantini. 1993. Isotopic patterns in modern global  
794 precipitation. In: P. K. Swart, J. McKenzie, K. C. Lohmann and S. Savin, editors, *Climate*  
795 *Change in Continental Isotopic Records*. American Geophysical Union, Washington DC. p.  
796 1-36.
- 797 Saxena, R.K. 1984. Seasonal variations of  $^{18}\text{O}$  in soil moisture and estimation of recharge in esker  
798 and moraine formations. *Nordic Hydrology* 15: 235-242.
- 799 Schneider, V. 2005. Apport de l'hydrodynamique et de la géochimie à la caractérisation des nappes  
800 de l'Oligocène et de l'Eocène, et à la reconnaissance de leurs relations actuelles et passées:  
801 origine de la dégradation de la nappe de l'Oligocène (sud-ouest du Bassin de Paris). PhD  
802 thesis, Université d'Orsay, Orsay, France.
- 803 Schoen, R., J.P. Gaudet and T. Bariac. 1999. Preferential flow and solute transport in a large  
804 lysimeter, under controlled boundary conditions. *Journal of Hydrology* 215: 70-81.  
805 doi:http://dx.doi.org/10.1016/S0022-1694(98)00262-5.
- 806 Song, X., S. Wang, G. Xiao, Z. Wang, X. Liu and P. Wang. 2009. A study of soil water movement  
807 combining soil water potential with stable isotopes at two sites of shallow groundwater areas  
808 in the North China Plain. *Hydrological Processes* 23: 1376-1388. doi:10.1002/hyp.7267.
- 809 Sprenger, M., D. Tetzlaff, J. Buttle, H. Laudon, H. Leister, C. Mitchell, et al. 2017. Measuring and  
810 modelling stable isotopes of mobile and bulk soil water. *Vadose Zone Journal*.  
811 doi:10.2136/vzj2017.08.0149. Sprenger, M., H. Leister, K. Gimbel and M. Weiler. 2016.  
812 Illuminating hydrological processes at the soil-vegetation-atmosphere interface with water  
813 stable isotopes. *Reviews of Geophysics* 54: 674-704. doi:10.1002/2015RG000515.
- 814 Sprenger, M., T.H.M. Volkmann, T. Blume and M. Weiler. 2015. Estimating flow and transport  
815 parameters in the unsaturated zone with pore water stable isotopes. *Hydrol. Earth Syst. Sci.*  
816 19: 2617-2635. doi:10.5194/hess-19-2617-2015.
- 817 Stumpp, C. and M.J. Hendry. 2012. Spatial and temporal dynamics of water flow and solute  
818 transport in a heterogeneous glacial till: The application of high-resolution profiles of  $\delta\text{O}-18$   
819 and  $\delta\text{H}-2$  in pore waters. *Journal of Hydrology* 438: 203-214.  
820 doi:10.1016/j.jhydrol.2012.03.024.
- 821 Stumpp, C. and P. Maloszewski. 2010. Quantification of preferential flow and flow heterogeneities  
822 in an unsaturated soil planted with different crops using the environmental isotope  $\delta^{18}\text{O}$ .  
823 *Journal of Hydrology* 394: 407-415. doi:10.1016/j.jhydrol.2010.09.014.
- 824 Stumpp, C., P. Maloszewski, W. Stichler and J. Fank. 2009a. Environmental isotope ( $\delta^{18}\text{O}$ ) and  
825 hydrological data to assess water flow in unsaturated soils planted with different crops: Case  
826 study lysimeter station "Wagna" (Austria). *Journal of Hydrology* 369: 198-208.  
827 doi:10.1016/j.jhydrol.2009.02.047.
- 828 Stumpp, C., W. Stichler and P. Maloszewski. 2009b. Application of the environmental isotope  
829  $\delta^{18}\text{O}$  to study water flow in unsaturated soils planted with different crops: Case study of a

- 830 weighable lysimeter from the research field in Neuherberg, Germany. *Journal of Hydrology*  
831 368: 68-78. doi:<http://dx.doi.org/10.1016/j.jhydrol.2009.01.027>.
- 832 Sutanto, S.J., J. Wenninger, A.M.J. Coenders-Gerrits and S. Uhlenbrook. 2012. Partitioning of  
833 evaporation into transpiration, soil evaporation and interception: a comparison between  
834 isotope measurements and a HYDRUS-1D model. *Hydrol. Earth Syst. Sci.* 16: 2605-2616.  
835 doi:10.5194/hess-16-2605-2012.
- 836 Thomas, E.M., H. Lin, C.J. Duffy, P.L. Sullivan, G.H. Holmes, S.L. Brantley, et al. 2013.  
837 Spatiotemporal Patterns of Water Stable Isotopic compositions at the Shale Hills Critical  
838 Zone Observatory: Linkages to Subsurface Hydrologic Processes. *Vadose Zone Journal* 12.  
839 doi:10.2136/vzj2013.01.0029.
- 840 Thornthwaite, C.W. 1948. An approach toward a rational classification of climate. *Geographical*  
841 *Review* 38: 55-94.
- 842 Turc, L. 1961. Estimation of irrigation water requirements, potential evapotranspiration: a simple  
843 climatic formula evolved up to date. *Annals of Agronomy* 12: 13:49.
- 844 Wei, Z., K. Yoshimura, L. Wang, D.G. Miralles, S. Jasechko and X. Lee. 2017. Revisiting the  
845 contribution of transpiration to global terrestrial evapotranspiration. *Geophysical Research*  
846 *Letters* 44: 2792-2801. doi:10.1002/2016GL072235.
- 847 Xu, C.Y. and D. Chen. 2005. Comparison of seven models for estimation of evapotranspiration and  
848 groundwater recharge using lysimeter measurement data in Germany. *Hydrological*  
849 *Processes* 19: 3717-3734. doi:10.1002/hyp.5853.
- 850
- 851

852 Figure captions

853

854 **Figure 1: Locations and photographs of the trenches where sand samples were taken for soil**  
855 **water extraction and water isotope analysis, for PB (a.) and for SLL (b.).**

856

857 **Figure 2: Monthly average oxygen isotopic composition of precipitation at PB (black) and**  
858 **SLL (grey). For each site, dashed lines represent the volume weighted average oxygen isotopic**  
859 **composition of the unsaturated zone profiles sampled in May 2006 for PB and May 2013 for**  
860 **SLL. Periods of recharge obtained from the water budget are represented by horizontal bars.**

861

862 **Figure 3: Time series of water and isotope surface budget for the PB site from 2002 to 2006:**  
863 **isotopic composition measured in precipitation (black and grey solid lines with monthly**  
864 **average as dashed lines), isotopic composition calculated in infiltrating water (red and**  
865 **orange), d-excess in precipitation (dashed grey line), measured precipitation (blue), calculated**  
866 **potential evapotranspiration (green) and infiltration into the unsaturated zone (red). See text**  
867 **for details.**

868

869

870 **Figure 4: Stable isotopic composition of water in precipitation (blue circles), in the**  
871 **unsaturated zone pore water (red triangles), and in groundwater (black square) for PB (a)**  
872 **and SLL (b). For each site, filled symbols correspond to volume weighted averages of**  
873 **individual empty data point. For each site, the Local Meteoric Water Lines (LMWL) and**  
874 **Global Meteoric Water Lines (GMWL) are represented by a black solid line and grey dashed**  
875 **line respectively.**

876

877 **Figure 5: Depth profiles of pore water oxygen isotopic composition (black) and volumetric**  
878 **water content (grey) at PB (a) and SLL (b). Vertical dashed lines correspond to volume**  
879 **weighted average isotopic composition in groundwater (black) and precipitation (blue).**  
880 **Annual or seasonal recharge is calculated through depth integration of water content in**  
881 **shaded areas. For PB, the modeled depth profile of isotopic composition (dashed line) is**  
882 **calculated from the hydro-isotopic surface budget and the 1D lumped parameter model (see**  
883 **text for details).**

884

885 **Figure 6: Depth profiles of lc-excess in pore water at PB (a) and SLL (b). For PB, the modeled**  
886 **depth profile of lc-excess (dashed line) is calculated from the hydro-isotopic surface budget**  
887 **and the 1D lumped parameter model (see text for details).**

888

889

890 Tables

891

892 **Table 1: Estimate of the amount of annual groundwater recharge at PB and SLL, using**  
893 **several methods. See text for details.**

894

	PB	SLL
UZ isotope profile	304 mm/yr	114 mm/yr
Hydro-isotopic water budget	203 mm/yr	200 - 370 mm/yr
Regional Modeling	150 mm/yr <sup>1</sup>	189 mm/yr <sup>2</sup>

895 <sup>1</sup> Corcho Alvarado et al. (2007)896 <sup>2</sup> Larocque et al. (2015)

897

898

899

900 **Table 2: Sensitivity analysis of the hydro-isotopic surface budget to the parameters  $Hr$ ,  $S_{max}$**   
901 **and  $f$ , and to potential evapotranspiration (PET) for PB. See text for details.**

	Average Recharge (mm)	$\delta^{18}\text{O}$ -weighted average (‰)	$\delta^2\text{H}$ -weighted average (‰)	lc-excess (‰)
Ref. case*	<b>203</b>	<b>-6.86</b>	<b>-50.00</b>	<b>-3.35</b>
$Hr = 0.1$	203	-6.95	-50.84	-3.55
$Hr = 0.5$	203	-6.72	-48.56	-2.90
$S_{max} \times 2$	147	-6.02	-46.31	-5.64
$S_{max} / 2$	231	-7.41	-52.52	-1.95
$f 0.99$	203	-8.13	-55.60	0.10
$f 0.90$	203	-2.52	-30.40	-14.65
PET +10%	192	-6.88	-50.16	-3.36
PET - 10%	217	-6.82	-49.75	-3.38
UZ profile (PB site)		<b>-6.86</b>	<b>-50.39</b>	-3.74

902 \* parameter values :  $S_{max} = 52$  mm,  $Hr=0.30$ ,  $f=0.97$ 

903

904

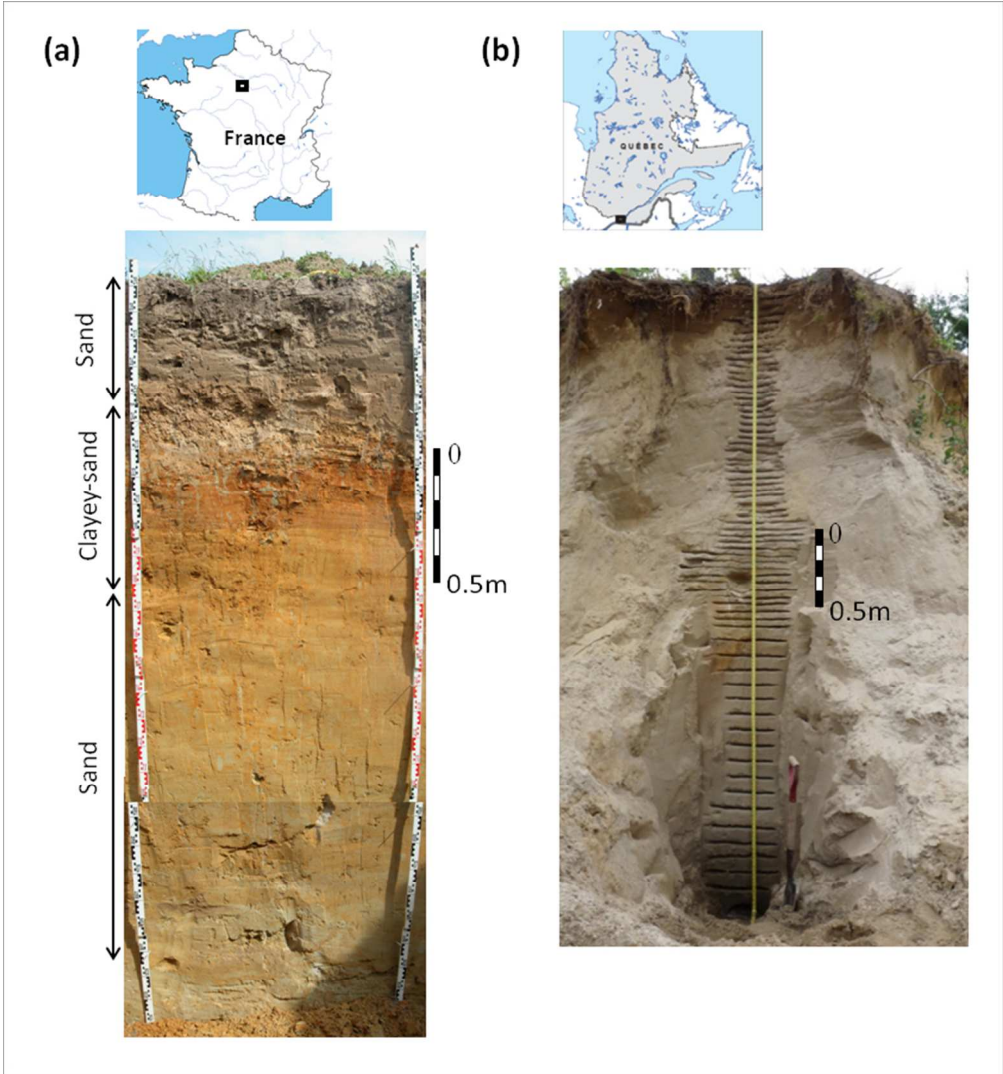


Figure 1: Locations and photographs of the trenches where sand samples were taken for soil water extraction and water isotope analysis, for PB (a.) and for SLL (b.).

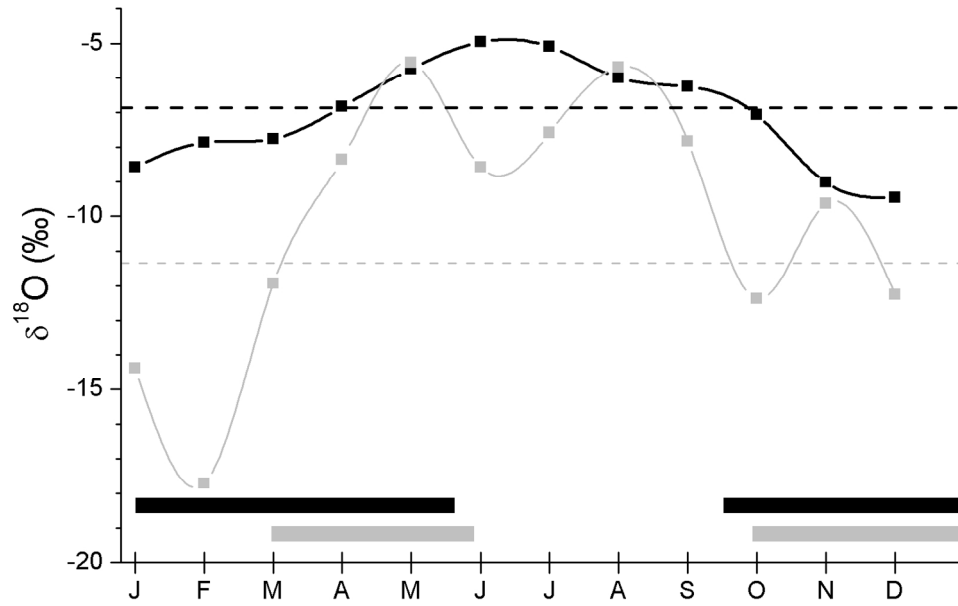


Figure 2: Monthly average oxygen isotopic composition of precipitation at PB (black) and SLL (grey). For each site, dashed lines represent the volume weighted average oxygen isotopic composition of the unsaturated zone profiles sampled in May 2006 for PB and May 2013 for SLL. Periods of recharge obtained from water budget are represented by horizontal bars.

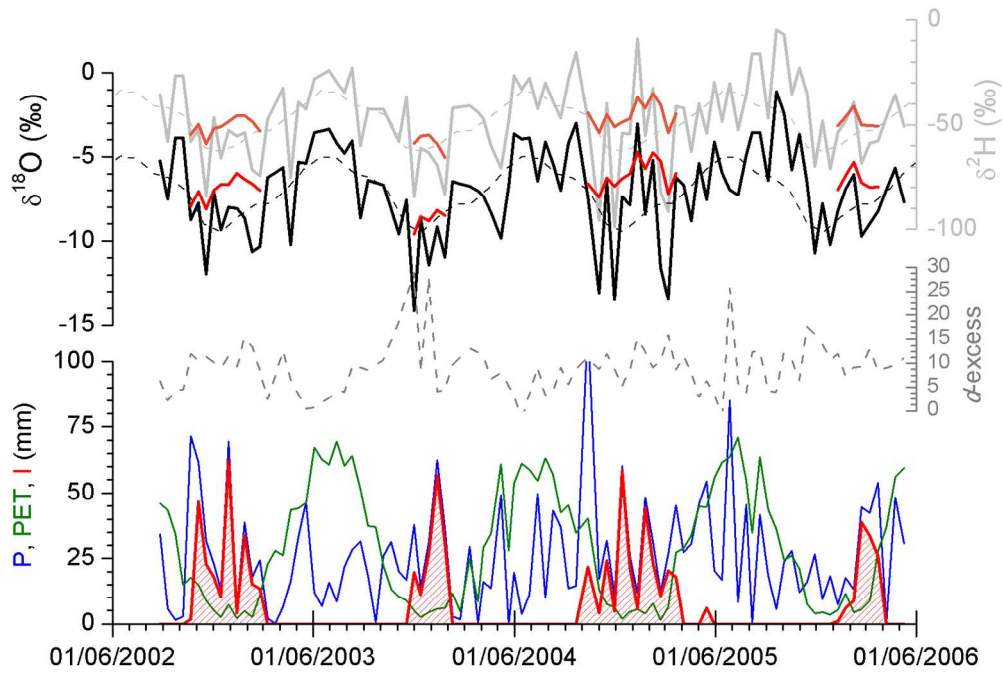


Figure 3: Time series of water and isotope surface budget for the PB site from 2002 to 2006: isotopic composition measured in precipitation (black and grey solid lines with monthly average as dashed lines), isotopic composition calculated in infiltrating water (red and orange), d-excess in precipitation (dashed grey line), measured precipitation (blue), calculated potential evapotranspiration (green) and infiltration into the unsaturated zone (red). See text for details.

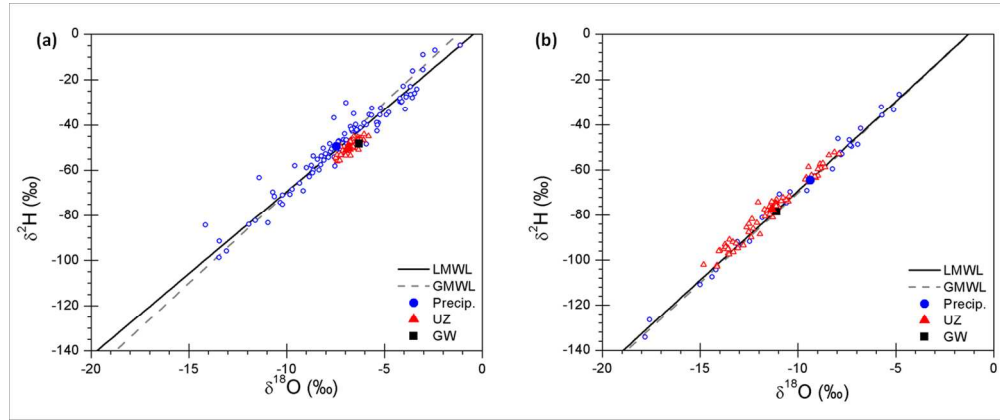


Figure 4: Stable isotopic composition of water in precipitation (blue circles), in the unsaturated zone pore water (red triangles), and in groundwater (black square) for PB (a) and SLL (b). For each site, filled symbols correspond to volume weighted averages of individual empty data point. For each site, the Local Meteoric Water Lines (LMWL) and Global Meteoric Water Lines (GMWL) are represented by a black solid line and grey dashed line respectively.



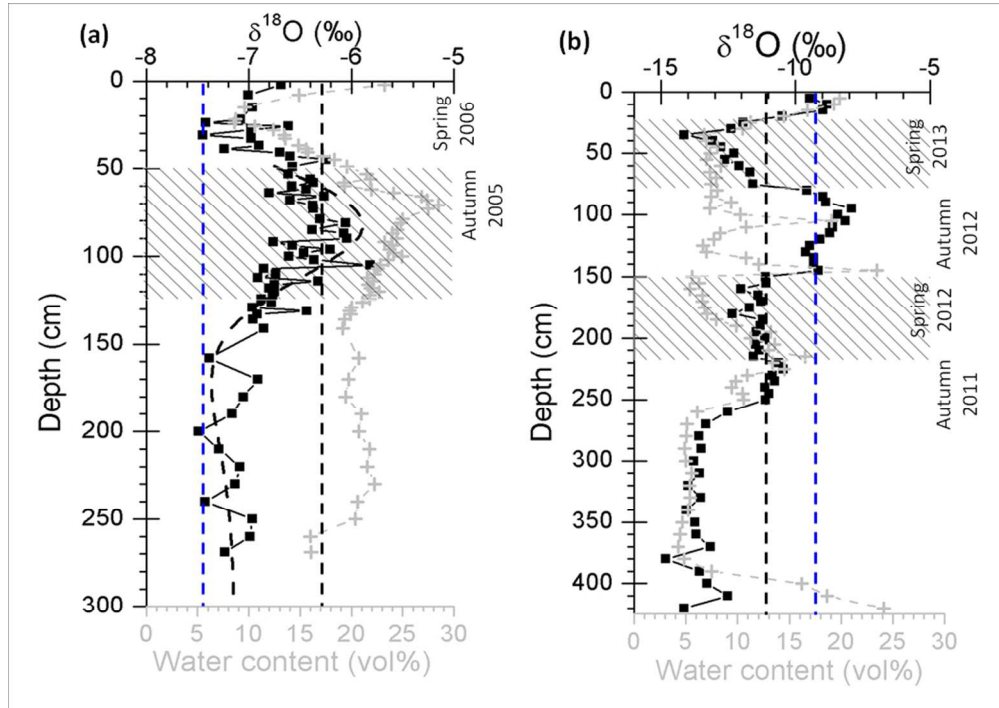


Figure 5: Depth profiles of pore water oxygen isotopic composition (black) and volumetric water content (grey) at PB (a) and SLL (b). Vertical dashed lines correspond to volume weighted average isotopic composition in groundwater (black) and precipitation (blue). Annual or seasonal recharge is calculated through depth integration of water content in shaded areas. For PB, the modeled depth profile of isotopic composition (dashed line) is calculated from the hydro-isotopic surface budget and the 1D lumped parameter model (see text for details).

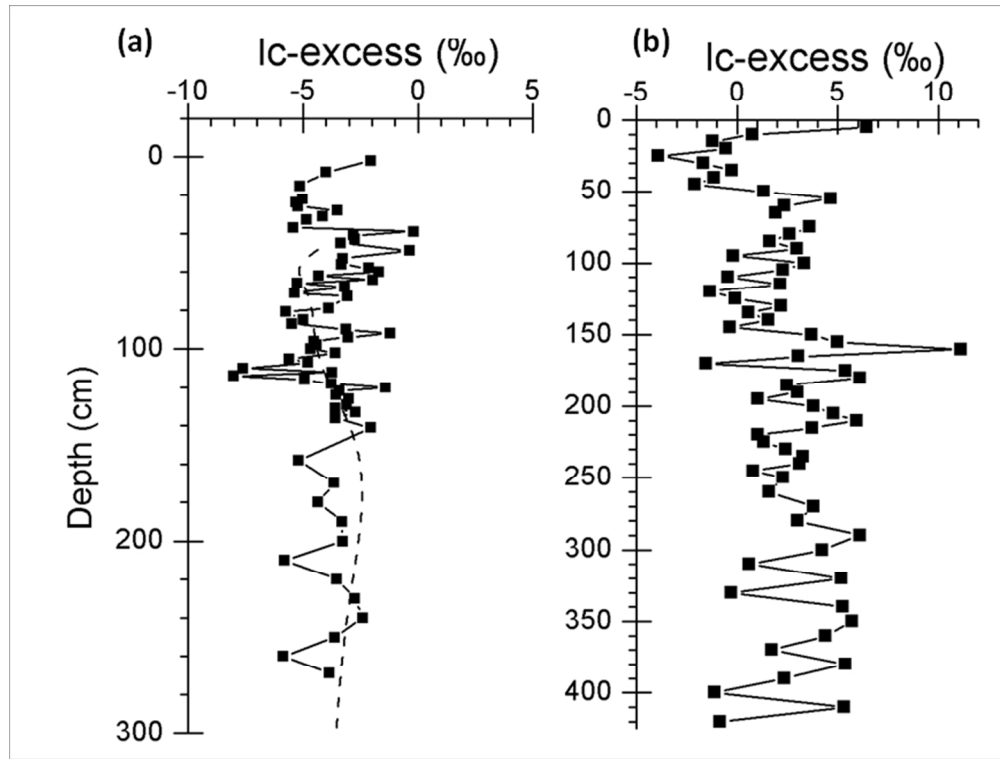


Figure 6: Depth profiles of Ic-excess in pore water at PB (a) and SLL (b). For PB, the modeled depth profile of Ic-excess (dashed line) is calculated from the hydro-isotopic surface budget and the 1D lumped parameter model (see text for details).